Mitigation of Magnus Force in Current-Induced Skyrmion Dynamics

Hiu Tung Fook, Wei Liang Gan, Indra Purnama, and Wen Siang Lew

School of Physical and Mathematical Sciences, Nanyang Technological University, Singapore 637371

Current-driven skyrmions drift from the intended direction of motion in a thin magnetic film due to the presence of the Magnus force and are annihilated upon reaching the film edge. This paper proposes two methods to engineer a 1-D potential well to confine the skyrmion motion in the center region of nanowires, thus preventing annihilation. By patterning the magnetic anisotropy of the film or by adding a layer of magnetic material at the edges, the barrier height and width of the potential well can be controlled. Magnetic skyrmions in such nanowires can then be guided to traverse only along the axis of the nanowire, even in the nanowires with steep bends. In addition, we also report a compression mechanism in which the skyrmion size and separation distance can be reduced by modifying the potential well, thus increasing the skyrmion packing density in a nanowire. The guided motion and high skyrmion density made possible by our proposed methods will allow the realization of high-density skyrmion-based memory.

Index Terms— **Magnetic skyrmions, micromagnetic simulations, perpendicular magnetic anisotropy (PMA), spin structures.**

I. Introduction

MAGNETIC skyrmions are stable magnetization configurations with integer topological numbers that have been recently found in materials with broken inversion symmetry. The presence of skyrmions in such materials is due to Dzyaloshinskii–Moriya interaction [1], [2]. Due to the topological configuration of skyrmions, they are shown to be much more resistant to pinning by defects when driven by current and can be driven under low applied current [3]–[6]. However, current-driven skyrmions drift from the direction of electron flow due to the presence of Magnus force, and this leads to annihilation at the magnetic film edge [7].

In this paper, we show that skyrmions can be guided along a nanowire without drifting away from the intended direction of motion by confining the skyrmions in the center region of the nanowire. This can be achieved by tuning of the perpendicular magnetic anisotropy (PMA) along the nanowire width or by creating a curbed nanowire.

II. Dynamics of Skyrmions Driven by In-Plane Current

The magnetization dynamics of skyrmions driven by in-plane current is expressed by the modified Landau–Lifshitz–Gilbert equation [8]–[10]

$$\tau = \frac{\gamma}{1+\alpha^2}(\mathbf{m}\times\mathbf{H}_{\text{eff}} + \alpha(\mathbf{m}\times(\mathbf{m}\times\mathbf{H}_{\text{eff}}))) + \tau_{ZL} \quad (1)$$

$$\tau_{ZL} = \frac{1}{1+\alpha^2}((1+\xi\alpha)\mathbf{m}\times(\mathbf{m}\times(u\cdot\nabla)\mathbf{m}) + (\xi-\alpha)\mathbf{m}\times(\mathbf{u}\cdot\nabla)\mathbf{m} \quad (2)$$

$$u = \frac{\mu_B}{2e\gamma M_{\text{sat}}(1+\xi^2)}\mathbf{j} \quad (3)$$

where $\mathbf{m}$ is the normalized unit vector of the local magnetization, γ is the electron gyromagnetic ratio, $\mathbf{H}_{\text{eff}}$ is the effective field, α is the Gilbert damping constant, e is the elementary charge, M_{sat} is the saturation magnetization, $\mathbf{j}$ is the current density vector, and ξ is the degree of the nonadiabacity.

Skyrmions are driven mostly by field-like torque from the spin-torque transfer (STT) and move at an angle toward the direction of electron flow when $\alpha \neq \xi$ [11]–[13]. This is due to the Magnus force caused by local magnetization and conduction electron coupling [7], [14]. The drift velocity of the skyrmion can be determined by

$$\mathbf{G}\times(\mathbf{v}_s - \mathbf{v}_d) + \mathbf{D}(\beta\mathbf{v}_s - \alpha\mathbf{v}_d) + \mathbf{F}_{\text{pin}} = 0 \quad (4)$$

where $\mathbf{v}_d$ is the drift velocity of the skyrmion, while $\mathbf{v}_s$ is the velocity of the conduction electron. The first term on the left-hand side of (4) is the Magnus force, with $\mathbf{G}$ as the gyromagnetic coupling vector; the second term is the dissipative force, with $\mathbf{D}$ as the dissipative force tensor; and the third term is the phenomenological pinning force ($\mathbf{F}_{\text{pin}}$) due to impurities; and β is the nonadiabatic constant of the STT [12].

III. Guided Skyrmion Motion in a Nanowire

A. Skyrmion Potential Well Generated by Magnetic Anisotropy Patterning

By tuning the magnetic anisotropy along the width of the nanowire, barriers can be formed to confine the skyrmions residing in the nanowire to within the center region. The effective field due to nanowire with a low anisotropy constant K in the center region is shown in Fig. 1(a). The effective field is much lower at the center region of the nanowire, allowing the magnetization to flip more easily. The lower magnetic anisotropy at the center, therefore, represents a path of lower resistance compared with the higher magnetic anisotropy at the edges.

Fig. 1(b) shows simulation snapshots of skyrmion motion in a nanowire with uniform magnetic anisotropy. At $t = 0.5$ ns, the skyrmion moves toward the edge due to Magnus force and at $t = 1$ ns, it starts to get annihilated. Fig. 1(c) shows snapshots of skyrmion motion in a nanowire with lower magnetic anisotropy at the center and higher magnetic anisotropy at the outer regions. Annihilation at the nanowire edge is prevented as the skyrmion is confined in the center region and moves along the intended direction. It has also been shown in the literature that the velocity of current-driven skyrmions is doubled by lowering the magnetic anisotropy of the center region from

Manuscript received March 19, 2015; revised April 25, 2015; accepted May 11, 2015. Date of publication May 14, 2015; date of current version October 22, 2015. Corresponding author: W. S. Lew (e-mail: wensiang@ntu.edu.sg).

Color versions of one or more of the figures in this paper are available online at http://ieeexplore.ieee.org.

Digital Object Identifier 10.1109/TMAG.2015.2433677

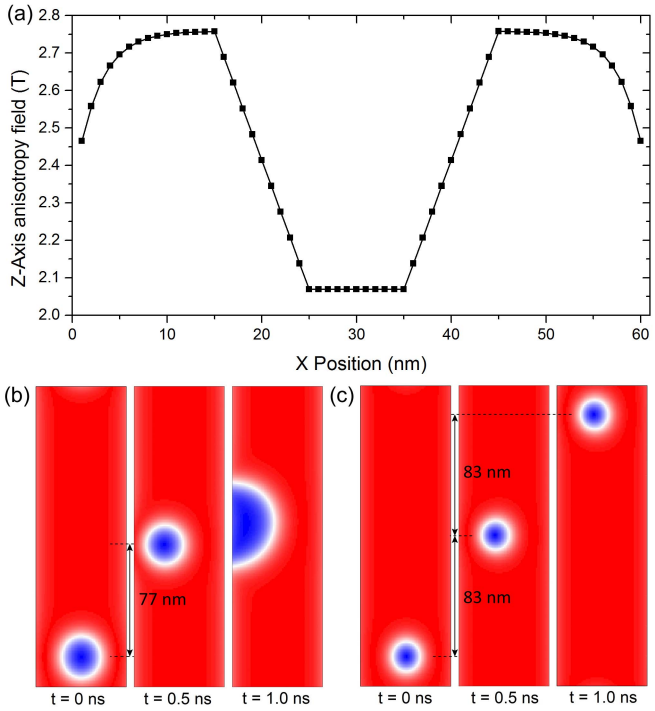

Fig. 1. (a) z-axis anisotropy field (T) along the width (nm) of the nanowire with a higher PMA of 8×10^5 J/m^3 at the outer region of the nanowire and a lower PMA of 6×10^5 J/m^3 at the 10 nm-wide center region, the gradient between the higher and lower PMA spans over 10 nm. The z-axis anisotropy field near the edges are lower due to the spin tilting near the nanowire edge. (b) Snapshots of simulation at times $t = 0$, 0.5 , and 1 ns of a skyrmion driven by current in a nanowire with uniform PMA of 6×10^5 J/m^3. (c) Snapshots of simulations of a skyrmion driven by current in a nanowire with tuned PMA to confine the skyrmion in the center region. Snapshot region is a 200 nm $\times$ 60 nm portion of an infinitely long nanowire.

8×10^5 to 6×10^5 J/m^3 [15]. The threshold skyrmion velocity at which annihilation would occur for uniform and patterned magnetic anisotropy is 130 and 250 m/s, respectively.

The PMA of Co/Pt multilayers can be patterned by light ion irradiation and accurately controlled by the fluence of the irradiation [16]. He^+ irradiation lowers the PMA of Co/Pt multilayers and when combined with high-resolution lithography, magnetic anisotropy patterning at nanometer scale can be achieved [17], [18]. Nucleation of skyrmions in the nonuniform PMA nanowire can be achieved with the application of a 2 ns spin polarized ($P = 0.7$) current of density 1.25×10^{12} A/m^2 in a circular region of diameter 20 nm at the center of the nanowire.

B. Engineering Skyrmion Potential Wells by Modifying Nanowire Geometry

The effect of nanowire geometry on current-induced skyrmion dynamics was also investigated. It was found that magnetic potential barriers can be formed by altering the nanowire geometry for the same purpose of confining the skyrmions to the center region of the nanowire.

The inset of Fig. 2 shows the 3-D model of the proposed curbed nanowire, which is created by an additional layer of material along both edges.

The z-axis demagnetization field acting on the magnetization along the width of both curbed and flat nanowires is shown in Fig. 2. In the curbed nanowire, there is a lower field at the center and a higher field at the inner edge of the curbs,

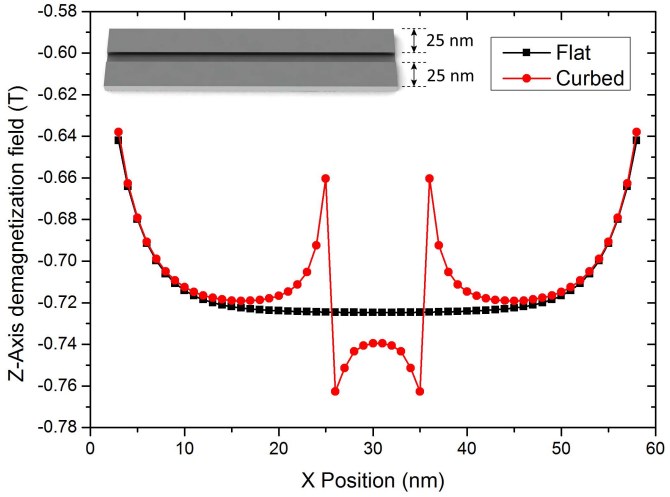

Fig. 2. z-axis demagnetization field (T) is higher at the inner edge of the curbs, thus confining skyrmions in the center region of the nanowire. The inset at the top-left shows the 3-D model of the curbed nanowire.

resulting in a magnetic potential well which confines the skyrmions residing in the nanowire to within the center region. In a flat nanowire, the skyrmion is confined only by the weak skyrmion-edge repulsion caused by the spin tilting at the nanowire edge [19]. The threshold skyrmion velocity of 660 m/s at which annihilation would occur for a curbed nanowire is significantly higher than PMA patterning due to topological repulsion from the curbs.

C. Guided Skyrmion Motion Along a U-Shaped Bend

The method of skyrmion confinement by a curbed nanowire was extended to form a curbed U-shaped nanowire. As the current density was higher at the inner radius of the bend, the width of the inner curb was reduced to 10 nm to maximize the driving of skyrmions along the bend by applied current. A 3-D model of the curbed U-shaped nanowire is shown in the inset of Fig. 5.

Fig. 3(a) and (b) shows the simulation snapshots of skyrmion motion driven by current density $j = 5 \times 10^{11}$ A/m^2 in a flat U-shaped and a curbed U-shaped nanowire, respectively. In the flat nanowire, the current-driven skyrmion moves toward the inner edge of the nanowire due to Magnus force and starts to get annihilated at $t = 0.9$ ns. However, in the curbed nanowire, the skyrmion enters the bend at $t = 0.4$ ns, travels along the bend, and exits at $t = 0.9$ ns, making an 180° turn. For both cases, the current density drives the skyrmion at a velocity of ~90 m/s in the straight portion of the nanowire.

IV. Operation Asymmetry

Although annihilation caused by the undesired skyrmion motion away from the direction of electron flow due to the Magnus force is prevented by the methods described in Section III, the presence of the Magnus force has an effect on the operation symmetry as it was observed that the dynamics of skyrmions travelling along the curbed U-shaped nanowire in the clockwise direction are different from those travelling in the anticlockwise direction.

Fig. 3(c) shows the position of a skyrmion travelling in the curbed U-shaped nanowire as a function of time for both clockwise and anticlockwise directions. Due to the curvature

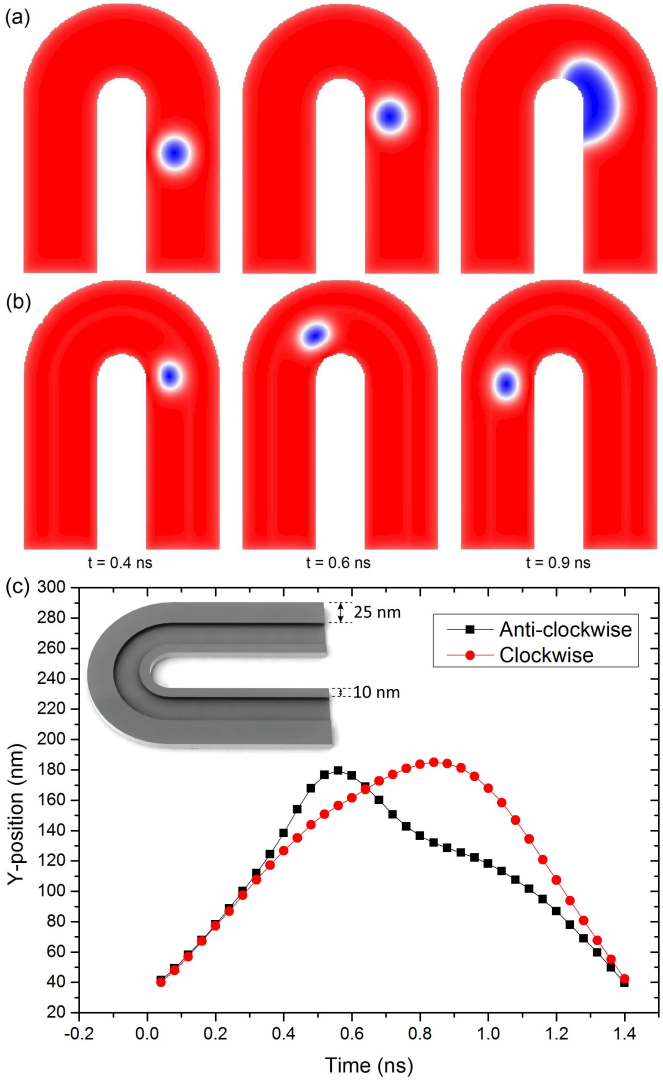

Fig. 3. Snapshots of simulations at different time. (a) Single skyrmion driven at current density of 5×10^{11} A/m^2 in the anticlockwise direction in a U-shaped nanowire with uniform thickness. (b) Single skyrmion driven at current density of 5×10^{11} A/m^2 in the anticlockwise direction in the curbed U-shaped nanowire. (c) Skyrmion y-position as a function of time for clockwise and anticlockwise directions. Inset: the 3-D model of the curbed U-shaped nanowire.

of the nanowire, the current density distribution is much higher in the inner radius. For a skyrmion travelling in the anticlockwise direction, it is driven to the inner edge of the nanowire and a skyrmion travelling in the clockwise direction is driven to the outer edge of the nanowire due to Magnus force. Skyrmions travelling in the anticlockwise direction accelerate upon entering the bend and overshoot into the outer region with lower current density. This causes the deceleration near the exit of the bend, the skyrmion then accelerates upon exiting the bend into the straight portion of the nanowire with higher current density. In traversing the bend, the current density provides a tangential force to counter the dissipative forces while the curb repulsions act as a centripetal force. The asymmetry results from the Magnus force, which can supplement or counter the curb repulsions depending on the direction of movement.

Fig. 4 shows that it is possible to drive more than one skyrmion along the curbed U-shaped nanowire. At $t = 0.4$ ns, the separation distance initially decreases

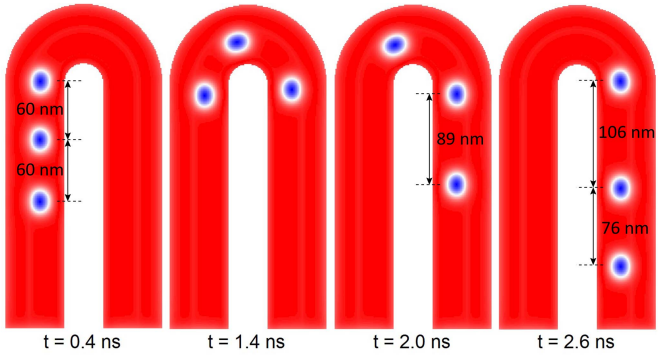

Fig. 4. Snapshots of simulation at times $t = 0.4, 1.4, 2$, and 2.6 ns of three skyrmions driven by current in the curbed U-shaped nanowire. Due to separation distances below the threshold, repulsion occurs at the exit of the bend between a skyrmion and a subsequent one. This increases the separation between the two skyrmions, a third skyrmion exiting the bend after the prior two would decrease the separation between the first two skyrmions but leaves a large separation from the second.

as the leading skyrmion entering the bend decelerates while the following skyrmion is traveling along the straight portion of the nanowire. At $t = 2$ ns, the separation distance then increases as the leading skyrmion exiting the bend accelerates while the following skyrmion is travelling along the bend.

A skyrmionic bit chain in a nanowire is not influenced by repulsions only when the spacing between skyrmions is larger than a certain threshold of ~60 nm as reported in [19]. Due to the increase and decrease in skyrmion velocity when entering and exiting the U-shaped bend, a minimum separation distance of ~100 nm before entering the bend is required to prevent any repulsion effect along the bend so that the separation does not deviate before and after the bend. As the repulsion force depends on the skyrmion size and separation distance, the minimum separation distance can be lowered by reducing skyrmion size.

V. Skyrmion Packing Density

Two skyrmions in a nanowire experience repulsion against each other with the repulsive force between two skyrmions described by

$$F_{ss} = K_1 \left(\frac{d\sqrt{H_k A}}{D} \right) \times \left(\frac{A}{t} \right) \tag{5}$$

where K_1 is the modified Bessel function, d is the distance between the centers of two skyrmions, H_k is the perpendicular anisotropy field, and A the exchange stiffness [19], [20]. As the force between two skyrmions, F_{ss}, is reduced due to smaller skyrmions size, the distance between their centers, d, is expected to decrease linearly with it.

It was observed that the skyrmion size can be reduced by a narrower center region due to the higher compression of skyrmions by the barriers. We can thus reduce the size of skyrmions in a nanowire by altering the width between barriers and increase the packing density of skyrmions in a nanowire.

Fig. 5 shows the relation of skyrmion size, equilibrium separation distance between two skyrmions and center region width. Due to smaller separation distance from reduced skyrmion sizes, the density is significantly increased when reducing barrier widths in the nanowire.

VI. Methods

Micromagnetic simulations were performed using MuMax3 [21], [22]. The material parameters used in the

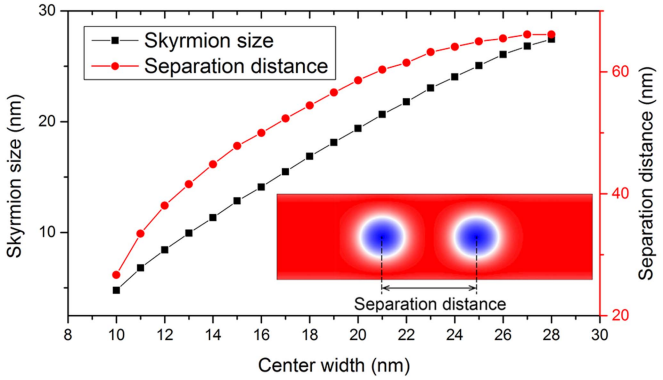

Fig. 5. Relation between skyrmion size, separation distance between two skyrmions in equilibrium, and center region width. Skyrmion sizes are measured by the diameter of the skyrmions. The inset at the bottom-right shows the separation distance measured from the center of both skyrmions.

TABLE I
MATERIAL PARAMETERS USED IN MICROMAGNETIC SIMULATIONS CORRESPONDING TO COBALT/PLATINUM MULTILAYERS

Symbol	Quantity	Value
M_{sat}	Saturation magnetization	580×10^3 A/m
K_U	Uniaxial anisotropy constant	6×10^5 J/m^3
D	Dzyaloshinskii-Moriya interaction strength	3×10^{-3} J/m^3
A	Exchange stiffness	15×10^{-12} J/m
ξ	STT non-adiabacity	0.35
α	Gilbert damping constant	0.1
P	Spin polarization	0.7

simulations correspond to that of Co/Pt multilayers, as shown in Table I [23], [24]. The nanowire thickness is $t_{\text{nanowire}} = 0.4$ nm and the width is $w_{\text{nanowire}} = 60$ nm. The width of the outer and inner curbs are $w_{\text{outer curb}} = 25$ nm and $w_{\text{inner curb}} = 10$ nm, respectively, with a thickness of $t_{\text{curb}} = 0.4$ nm.

VII. CONCLUSION

We showed two methods to confine skyrmions residing in a nanowire to prevent annihilation due to the Magnus force that drives the skyrmions to the nanowire edge when driven by in-plane current. By tuning the magnetic anisotropy along the width of the nanowire or by creating a curbed nanowire, skyrmions are confined in the center region and can be guided along the nanowire shape. We showed that skyrmion motion can be guided along a curbed U-shaped nanowire and that several skyrmions can be driven along the nanowire at small separation distances between them. We have, therefore, demonstrated for the first time the possibility of passive skyrmion guiding. This solves the long standing issue of skyrmion annihilation due to the Magnus force. We also showed that by reducing the width between the barriers in the nanowire, the size of skyrmions can be reduced and results in smaller separation distances, significantly increasing the packing density of skyrmions in a nanowire. The combination of guided skyrmion motion along nanowires and efficient manipulation of skyrmion size by the proposed methods will be beneficial to the creation of high-density skyrmion-based memory devices.

ACKNOWLEDGMENT

This work was supported by the Singapore National Research Foundation within the Competitive Research Programme Non-Volatile Magnetic Logic and Memory Devices under Grant NRF-CRP009-2011-01. The authors wish to acknowledge the funding support for this project from Nanyang Technological University under the Undergraduate Research Experience on CAmpus (URECA) Programme.

REFERENCES

[1] A. Fert and P. M. Levy, "Role of anisotropic exchange interactions in determining the properties of spin-glasses," *Phys. Rev. Lett.*, vol. 44, no. 23, pp. 1538–1541, 1980.
[2] A. Fert, "Magnetic and transport properties of metallic multilayers," *Mater. Sci. Forum*, vols. 59–60, pp. 439–480, Jan. 1990.
[3] N. Nagaosa and Y. Tokura, "Topological properties and dynamics of magnetic skyrmions," *Nature Nanotechnol.*, vol. 8, pp. 899–911, Dec. 2013.
[4] J. Sampaio, V. Cros, S. Rohart, A. Thiaville, and A. Fert, "Nucleation, stability and current-induced motion of isolated magnetic skyrmions in nanostructures," *Nature Nanotechnol.*, vol. 8, pp. 839–844, Oct. 2013.
[5] A. Fert, V. Cros, and J. Sampaio, "Skyrmions on the track," *Nature Nanotechnol.*, vol. 8, pp. 152–156, Mar. 2013.
[6] X. Z. Yu *et al.*, "Skyrmion flow near room temperature in an ultralow current density," *Nature Commun.*, vol. 3, Aug. 2012, Art. ID 988.
[7] J. Iwasaki, M. Mochizuki, and N. Nagaosa, "Current-induced skyrmion dynamics in constricted geometries," *Nature Nanotechnol.*, vol. 8, pp. 742–747, Sep. 2013.
[8] J. C. Slonczewski, "Current-driven excitation of magnetic multilayers," *J. Magn. Magn. Mater.*, vol. 159, nos. 1–2, pp. L1–L7, 1996.
[9] J. Xiao, A. Zangwill, and M. D. Stiles, "Boltzmann test of Slonczewski's theory of spin-transfer torque," *Phys. Rev. B*, vol. 70, no. 17, p. 172405, Nov. 2004.
[10] S. Zhang and Z. Li, "Roles of nonequilibrium conduction electrons on the magnetization dynamics of ferromagnets," *Phys. Rev. Lett.*, vol. 93, p. 127204, Sep. 2004.
[11] A. Brataas, A. D. Kent, and H. Ohno, "Current-induced torques in magnetic materials," *Nature Mater.*, vol. 11, pp. 372–381, Apr. 2012.
[12] A. Thiaville, Y. Nakatani, J. Miltat, and Y. Suzuki, "Micromagnetic understanding of current-driven domain wall motion in patterned nanowires," *Europhys. Lett.*, vol. 69, no. 6, p. 990, 2005.
[13] Y. Zhou and M. Ezawa, "A reversible conversion between a skyrmion and a domain-wall pair in a junction geometry," *Nature Commun.*, vol. 5, Aug. 2014, Art. ID 4652.
[14] T. Schulz *et al.*, "Emergent electrodynamics of skyrmions in a chiral magnet," *Nature Phys.*, vol. 8, pp. 301–304, Feb. 2012.
[15] J. Ding, X. Yang, and T. Zhu, "Manipulating current induced motion of magnetic skyrmions in the magnetic nanotrack," *J. Phys. D, Appl. Phys.*, vol. 48, no. 11, p. 115004, 2015.
[16] C. Chappert *et al.*, "Planar patterned magnetic media obtained by ion irradiation," *Science*, vol. 280, no. 5371, pp. 1919–1922, 1998.
[17] T. Devolder *et al.*, "Sub-50 nm planar magnetic nanostructures fabricated by ion irradiation," *Appl. Phys. Lett.*, vol. 74, no. 22, pp. 3383–3385, 1999.
[18] T. Devolder *et al.*, "Patterning of planar magnetic nanostructures by ion irradiation," *J. Vac. Sci. Technol. B, Microelectron. Nanometer Struct.*, vol. 17, no. 6, pp. 3177–3181, 1999.
[19] X. Zhang *et al.*, "Skyrmion-skyrmion and skyrmion-edge repulsions in skyrmion-based racetrack memory," *Sci. Rep.*, vol. 5, Jan. 2015, Art. ID 7643.
[20] S.-Z. Lin, C. Reichhardt, C. D. Batista, and A. Saxena, "Particle model for skyrmions in metallic chiral magnets: Dynamics, pinning, and creep," *Phys. Rev. B*, vol. 87, p. 214419, Jun. 2013.
[21] A. Vansteenkiste *et al.*, "The design and verification of MuMax3," *AIP Adv.*, vol. 4, no. 10, p. 107133, 2014.
[22] M. Najafi *et al.*, "Proposal for a standard problem for micromagnetic simulations including spin-transfer torque," *J. Appl. Phys.*, vol. 105, no. 11, p. 113914, 2009.
[23] A. Barman, S. Wang, O. Hellwig, A. Berger, E. E. Fullerton, and H. Schmidt, "Ultrafast magnetization dynamics in high perpendicular anisotropy $[Co/Pt]_n$ multilayers," *J. Appl. Phys.*, vol. 101, no. 9, p. 09D102, 2007.
[24] P. J. Metaxas *et al.*, "Creep and flow regimes of magnetic domain-wall motion in ultrathin Pt/Co/Pt films with perpendicular anisotropy," *Phys. Rev. Lett.*, vol. 99, p. 217208, Nov. 2007.